

## The Effect of Chemical Composition and Electrolyte Temperature on the Size and Structure of Cadmium Sulfide Nanocrystals Obtained by the Electrolytic Method

N.B. Danilevska<sup>1</sup>, M.V. Moroz<sup>2,3,\*</sup>, B.D. Nechyporuk<sup>1</sup>, S.H. Haievska<sup>4</sup>, M.Yu. Novoseletskyi<sup>1</sup>,  
M.V. Prokhorenko<sup>5</sup>, N.P. Yarema<sup>5</sup>, V.O. Yukhymchuk<sup>6</sup>, Fiseha Tesfaye<sup>7</sup>, O.V. Reshetnyak<sup>3</sup>

<sup>1</sup> Rivne State University of Humanities, 31, Plastova St., 33000 Rivne, Ukraine

<sup>2</sup> National University of Water and Environmental Engineering, 11, Soborna St., 33028 Rivne, Ukraine

<sup>3</sup> Ivan Franko National University of Lviv, 6, Kyrylo i Mefodiy St., 79005 Lviv, Ukraine

<sup>4</sup> Rivne Research Forensic Center, 39, Gagarina St., 33033 Rivne, Ukraine

<sup>5</sup> Lviv Polytechnic National University, 12, S. Bandery St., 79013 Lviv, Ukraine

<sup>6</sup> V.Ye. Lashkaryov Institute of Semiconductors Physics, National Academy of Sciences of Ukraine,  
41, Prosp. Nauky, 03028 Kyiv, Ukraine

<sup>7</sup> Åbo Akademi University, Johan Gadolin Process Chemistry Centre, 8, Piispankatu St., 20500 Turku, Finland

(Received 27 April 2020; revised manuscript received 15 August 2020; published online 25 August 2020)

Cadmium sulfide (CdS) nanocrystals were produced by the electrolytic method in a glass electrolyzer with cadmium electrodes. Solutions of sodium thiosulfate ( $\text{Na}_2\text{S}_2\text{O}_3$ ), sodium sulfite ( $\text{Na}_2\text{SO}_3$ ) and sodium sulfide ( $\text{Na}_2\text{S}$ ) in distilled water were used as electrolytes. It was determined that the composition of the obtained phases depends on the electrolyte and the synthesis temperature. Cadmium sulfide as a single-phase reaction product was obtained from  $\text{Na}_2\text{S}_2\text{O}_3$  and  $\text{Na}_2\text{S}$  solutions at  $T = 371$  K. The use of other electrolytes and temperatures yields additional phases  $\text{CdCO}_3$  and Cd, besides CdS. The size of the synthesized nanoparticles and their crystal structure were evaluated from XRD data using Debye-Scherrer and Williamson-Hall formulae. The size of CdS nanoparticles decreases as the temperature of sodium thiosulfate solution lowers from  $T = 371$  K to  $T = 292$  K. The values of mechanical stress were calculated for the cubic and hexagonal modifications of CdS nanocrystals. Raman spectra of cadmium sulfide nanocrystals obtained from sodium thiosulfate solution were investigated. Scattering bands at frequency positions  $302\text{ cm}^{-1}$ ,  $603\text{ cm}^{-1}$ , and  $900\text{ cm}^{-1}$ , with monotonously decreasing intensity, were recorded. Detailed analysis of produced experimental results and reported literature data was undertaken. It was established that the phase transition from the cubic sphalerite to hexagonal wurtzite takes place during the annealing of nanocrystals at  $T = 773$  K. The phase transition results in increased size and lower mechanical stress in cadmium sulfide nanocrystals.

**Keywords:** Cadmium sulfide, X-ray structural studies, Nanoparticle size, Raman spectroscopy.

DOI: [10.21272/jnep.12\(4\).04035](https://doi.org/10.21272/jnep.12(4).04035)

PACS numbers: 61.46.Df, 61.82.Fk, 61.05.C, 33.20.Fb

### 1. INTRODUCTION

Cadmium sulfide (CdS) is a wide-gap semiconductor. Its properties change substantially upon the transition from macro-sized samples to nanostructured state. For instance, the bandgap of CdS single crystals at room temperature is 2.4 eV but can reach up to 4.5 eV for CdS nanocrystals [1, 2]. CdS nanoparticles exhibit non-linear dependence of luminescence emission frequency on the particle size, and thus can be used as quantum dots for biological object imaging and development of new optoelectronic devices [3, 4]. Additionally, unique photoconductivity and luminescent properties make CdS a material for manufacturing injection lasers, solar cells, photosensors, photoresistors, scintillation detectors of elementary particles and  $\gamma$ -radiation etc. [5].

CdS crystallizes in either cubic (sphalerite) or hexagonal (wurtzite) structure. The sphalerite structure with the lattice parameter  $a = 0.58250$  nm is stable at low temperatures. High-temperature hexagonal CdS has lattice periods  $a = 0.41368$  nm,  $c = 0.67163$  nm. The temperature of the polymorphous sphalerite-wurtzite transition depends substantially on the sample size. For instance, the transition in a bulk material takes place in the range of  $T = 973$ - $1073$  K. The phase transition in

nanoparticles is observed after annealing at  $T \sim 820$  K [6]. Depending on the synthesis conditions, the color of CdS may vary from golden yellow to reddish yellow.

Various approaches to nanocrystal synthesis were investigated, such as vacuum deposition, chemical bath deposition, pyrolysis, sol-gel method, etc. [2, 7, 8]. For instance, chemical bath can be used for commercial production of thin films on metal, semiconductor, and insulator substrates, as a relatively inexpensive, convenient and simple method. A specific of this method, and sometimes the drawback, is that aqueous solutions, in addition to the principal reaction, sometimes undergo reactions with the formation of metal oxides [9].

Electrolytic synthesis of nanoparticles also belongs to the methods of chemical bath deposition but uses anode dissolution of metallic electrodes as a source of metal ions. Techniques of the nanocrystal synthesis of cadmium sulfide and zinc sulfide from sodium thiosulfate solution were reported in [10, 11]. The effect of electrolyte composition on the processes of the nanoparticle production of zinc compounds was studied in [12].

The purpose of this work is to investigate the effect of chemical composition and temperature of the electrolyte on the synthesis of nanoparticles of cadmium compounds, including CdS.

\* [m.v.moroz@nuwm.edu.ua](mailto:m.v.moroz@nuwm.edu.ua)

## 2. EXPERIMENTAL

CdS nanocrystals were obtained by the electrolytic method in a 1000 ml glass two-electrode electrolyzer. Cylindrical electrodes of 7.5 mm diameter and 180 mm length were prepared from high-purity cadmium. Solutions of  $\text{Na}_2\text{S}_2\text{O}_3 \cdot 5\text{H}_2\text{O}$  ( $m = 10.00$  g),  $\text{Na}_2\text{SO}_3$  ( $m = 9.29$  g) and  $\text{Na}_2\text{S} \cdot 9\text{H}_2\text{O}$  ( $m = 19.35$  g) in 800 ml of distilled water were prepared as electrolytes. Under these conditions, the solution concentration  $c$  of sodium thiosulfate ( $\text{Na}_2\text{S}_2\text{O}_3$ ), sodium sulfite ( $\text{Na}_2\text{SO}_3$ ) and sodium sulfide ( $\text{Na}_2\text{S}$ ) was 12.50, 11.61, and 24.19 g/l, respectively. The electrolysis conditions were: electrolyte temperature  $T = 292$  K or  $T = 371$  K, synthesis duration  $t = 2-3$  h, voltage between electrodes  $U \sim 10$  V, and current density  $j = 7.0 \cdot 10^{-3}$  A/cm<sup>2</sup>. Such level of the current density does not cause heating of the electrolyte during the process. The electrolyzer was powered by a stabilized source of direct current IEPP-2. To ensure uniform use of the electrode material, the direction of current was changed every 30 min. At the end of the process, the electrolyte was filtered at a paper filter, and the obtained powder was washed by a five-fold (vs. the electrolyte) volume of distilled water. The precipitates as nanocrystal aggregates were air-dried at room temperature. After the electrolysis, the mass change of cadmium electrodes and the mass of the obtained powder were determined.

X-ray studies utilized a DRON-4 diffractometer using  $\text{CuK}_\alpha$  radiation ( $\lambda = 0.154060$  nm) at room temperature. Diffraction patterns were recorded using Bragg-Brentano scheme ( $\theta$ - $2\theta$ ), scan step  $0.05^\circ$  and 5 s exposure at each point.

Raman spectra were recorded on a Dilor XY 800 spectrometer using an  $\text{Ar}^+$  laser at 80 mW power at a wavelength  $\lambda = 514.5$  nm equipped with multichannel detection, backscattering geometry.

For the analysis of experimental diffraction patterns, each reflection was described by a Gaussian function to obtain information about the angular position  $2\theta$ , full width at half-maximum  $\beta$  (FWHM), integral intensity  $I$ . Similar calculations were performed for any compounds that formed during the electrolytic synthesis.

## 3. RESULTS AND DISCUSSION

X-ray diffraction patterns of samples obtained from sodium thiosulfate solution at various temperatures are shown in Fig. 1. It was determined that the electrolyte temperature greatly affects the color of the synthesized material. Specifically, the nanocrystals obtained at  $T = 371$  K have red color, and those produced at  $T = 292$  K are yellow-red.

Diffraction pattern (Fig. 1a) has four wide reflections at  $2\theta$  angles  $26.9^\circ$ ,  $44.4^\circ$ ,  $52.0^\circ$ , and  $71.3^\circ$ . The angular positions of X-ray reflections were calculated using Wolf-Bragg formula. It was established that the cubic modification is formed under these synthesis conditions, and the reflections identified in Fig. 1a correspond to Miller indices (1 1 1), (2 2 0), (3 1 1), and (3 3 1), respectively. Large reflection FWHM indicates the small size of the crystals. Similar results were reported in [10] for CdS nanocrystals obtained by the electrolytic method from sodium thiosulfate solution with  $c = 74.3$  g/l.

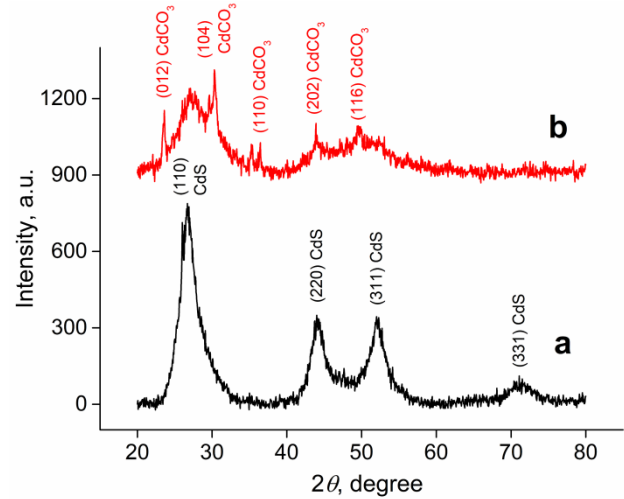


**Fig. 1** – Diffraction patterns of samples obtained by electrolytic method:  $t = 2$  h, electrolyte is  $\text{Na}_2\text{S}_2\text{O}_3$  solution ( $c = 12.50$  g/l) at  $T = 371$  K (a) and  $T = 292$  K (b)

The size of the obtained nanocrystals  $D$  was calculated using Debye-Scherrer formula [13]:

$$D = 0.89\lambda/(\beta \cdot \cos\theta), \quad (3.1)$$

where  $\lambda$  is the X-ray radiation wavelength;  $\beta$  is the FWHM reflection;  $\theta$  is the diffraction angle.

The reflection width values were determined by the formula:

$$\beta = (\beta_1^2 - \beta_2^2)^{1/2}, \quad (3.2)$$

where  $\beta_1$ ,  $\beta_2$  are the experimental and instrumental components of FWHM, respectively.

Instrumental share of the reflection width was calculated from the diffraction patterns of silicon and  $\text{Al}_2\text{O}_3$  powder standards obtained under the same conditions as this experiment.

The values of  $D$  calculated from Eq. (3.1) differ for each identified reflection, and their average is  $\sim 3.0$  nm. It was established that the value of the instrumental parameter  $\beta_2$  has practically no effect on the obtained results. This is due to the fact that the experimental component far exceeds the instrumental one.

According to Eq. (3.1), the X-ray reflection width  $\beta$  is inversely proportional to the particle size  $D$ . The magnitude of  $\beta$  is also affected by mechanical stress caused by defects in the crystal structure. The structure defects are particularly pronounced in the nanoparticles where many of the atoms are on the surface, and the contribution of surface atoms is significantly greater.

The size and mechanical stress in CdS nanocrystals can also be calculated by Williamson-Hall method [13]. The value of  $\beta$  in this method is described as:

$$\beta = 0.89\lambda/(D \cdot \cos\theta) + 4\varepsilon \cdot \text{tg}\theta, \quad (3.3)$$

where  $\varepsilon$  is the relative elongation of the sample.

The first term of Eq. (3.3) describes the contribution of dimensional effect to the value of  $\beta$ , and the second term is the contribution of mechanical stress.

We rewrite Eq. (3.3) in the form of:

$$\beta \cdot \cos\theta = 0.89\lambda/D + 4\varepsilon \cdot \sin\theta. \quad (3.4)$$

According to Hooke's law, mechanical stress  $\sigma$  under elastic deformations is related to Young's modulus  $E$  as:

$$\sigma = E \cdot \varepsilon. \quad (3.5)$$

Having determined the value of  $\varepsilon$  from Eq. (3.5) and substituting it in Eq. (3.4), we obtain:

$$\beta \cdot \cos\theta = 0.89\lambda/D + 4\sigma \sin\theta/E. \quad (3.6)$$

Analyzing Eq. (3.6), we can conclude that the plot in the coordinate system  $\beta \cdot \cos\theta = f(4\sin\theta/E)$  is a straight line. Therefore, the values of  $D$  and  $\sigma$  can be calculated from the coefficients of the linear dependence.

Young's modulus  $E$  for single crystals depends on the crystallographic direction, i.e. Miller indices  $(h k l)$  and the crystal structure. This dependence for the cubic and hexagonal structures, respectively, is described by the formulae:

$$E^{-1} = S_{11} - \frac{(2S_{11} - 2S_{12} - S_{44})(h^2k^2 + k^2l^2 - l^2h^2)}{(h^2 + k^2 + l^2)^2} \quad (3.7)$$

and

$$E^{-1} = \frac{(h^2 + k^2 - hk)^2 a^4 S_{11} + l^4 c^4 S_{33} + (h^2 + k^2 - hk)l^2 a^2 c^2 (S_{44} + 2S_{13})}{[(h^2 + k^2 - hk)a^2 + l^2 c^2]^2}, \quad (3.8)$$

where  $S_{11}$ ,  $S_{12}$ ,  $S_{13}$ ,  $S_{33}$ , and  $S_{44}$  are the coefficients of elastic yield;  $a$  and  $c$  are the lattice parameters.

Using elastic yield coefficients for the cubic modification of CdS:  $S_{11} = 30.7 \cdot 10^{-12} \text{ Pa}^{-1}$ ,  $S_{12} = -12.5 \cdot 10^{-12} \text{ Pa}^{-1}$ ,  $S_{44} = 42.4 \cdot 10^{-12} \text{ Pa}^{-1}$  [14], and the previously determined Miller indices for reflections in Fig. 1a, the values of  $E$  for various directions in the single crystals were calculated. Similar calculations were performed for the hexagonal modification, taking into account the elastic yield coefficients  $S_{11} = 20.8 \cdot 10^{-12} \text{ Pa}^{-1}$ ,  $S_{13} = -5.4 \cdot 10^{-12} \text{ Pa}^{-1}$ ,  $S_{33} = 16.0 \cdot 10^{-12} \text{ Pa}^{-1}$ ,  $S_{44} = 66.6 \cdot 10^{-12} \text{ Pa}^{-1}$ , and the unit cell parameters  $a = 0.41367 \text{ nm}$ ,  $c = 0.67161 \text{ nm}$  [14].

The  $\beta \cdot \cos\theta = f(4\sin\theta/E)$  dependence for CdS nanocrystals obtained at the electrolyte temperature  $T = 371 \text{ K}$  is plotted in Fig. 2. The nanocrystal size and mechanical stress value (tensile stress) calculated by Williamson-Hall method are  $3.4 \text{ nm}$  and  $1.6 \cdot 10^8 \text{ Pa}$ , respectively.

The diffraction pattern in Fig. 1b has, in addition to the wide reflections, also some narrow reflections at  $2\theta$  angles  $23.5^\circ$ ,  $30.2^\circ$ ,  $35.3^\circ$ ,  $36.6^\circ$ ,  $43.8^\circ$ , and  $49.4^\circ$ , that are characteristic of cadmium carbonate ( $\text{CdCO}_3$ ) [10]. Cadmium carbonate is formed due to the presence of carbon dioxide dissolved in distilled water. Therefore, lowering the electrolyte temperature from  $T = 371 \text{ K}$  to  $T = 292 \text{ K}$ , with other synthesis conditions being equal, yields nanocrystals of CdS and  $\text{CdCO}_3$ .

The nanocrystal size of CdS and  $\text{CdCO}_3$  calculated by Debye-Scherrer method is  $1.6 \text{ nm}$  and  $25 \text{ nm}$ , respectively. The values for CdS calculated by Williamson-Hall method are  $D = 2.0 \text{ nm}$  and  $\sigma = 5.1 \cdot 10^8 \text{ Pa}$ . Therefore, the dimensions of CdS nanocrystals obtained at  $T = 292 \text{ K}$  are reasonably close for both calculations. Additionally, we can observe that the particle size  $D$  decreases as the electrolyte temperature drops from  $T = 371 \text{ K}$  to  $T = 292 \text{ K}$ .

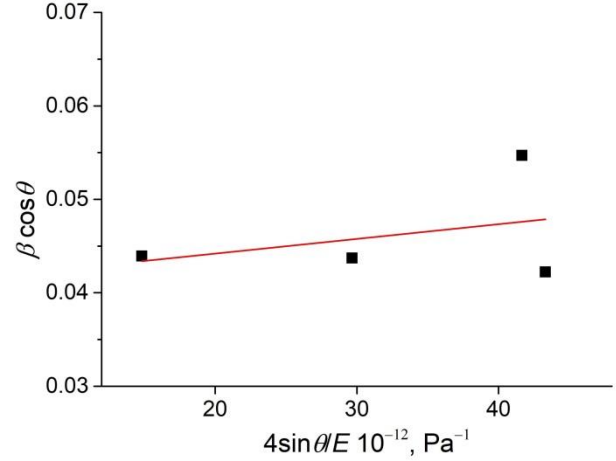


Fig. 2 – The  $\beta \cdot \cos\theta = f(4\sin\theta/E)$  dependence for CdS nanocrystals obtained at  $T = 391 \text{ K}$

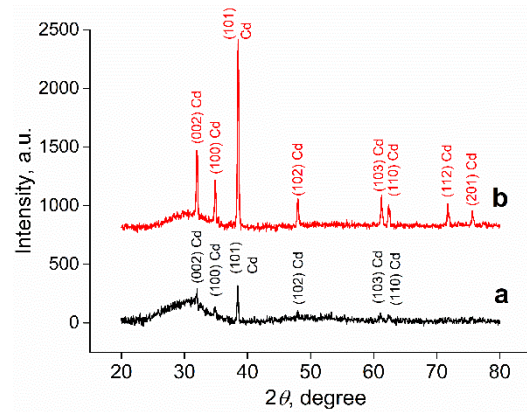
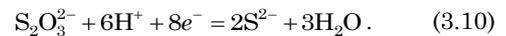
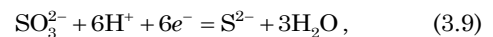


Fig. 3 – Diffraction patterns of samples obtained by electrolytic method:  $t = 2 \text{ h}$ , electrolyte is  $\text{Na}_2\text{SO}_3$  solution ( $c = 11.61 \text{ g/l}$ ) at  $T = 371 \text{ K}$  (a) and  $T = 292 \text{ K}$  (b)

X-ray diffraction patterns of nanocrystals obtained with sodium sulfite solution as the electrolyte are shown in Fig. 3. Similarly to Fig. 1, wide reflections typical of CdS nanocrystals were identified. Additionally, Fig. 3b features narrow reflections at  $2\theta$  angles  $32.2^\circ$ ,  $35.0^\circ$ ,  $38.4^\circ$ ,  $48.1^\circ$ ,  $61.1^\circ$ ,  $62.3^\circ$ ,  $71.4^\circ$ , and  $75.6^\circ$ , which are characteristic of metallic cadmium. The intensity of the latter in Fig. 3a is substantially lower. The dimensions of CdS and Cd nanocrystals determined by Debye-Scherrer method were  $1.3 \text{ nm}$ ,  $63.6 \text{ nm}$  (at  $T = 371 \text{ K}$ ) and  $1.2 \text{ nm}$ ,  $66.7 \text{ nm}$  (at  $T = 292 \text{ K}$ ), respectively.

The formation of CdS from sodium sulfite and thio-sulfate solutions occurs after the change of the electrode polarity. Specifically, during the cathode polarization of the working electrode the respective anions are reduced to sulfide  $\text{S}^{2-}$  according to reactions (3.9) and (3.10):



The standard electrode potentials  $E$  of half-reactions (3.9) and (3.10) are  $0.231 \text{ V}$  and  $-0.006 \text{ V}$ , respectively [15].

The formed sulfide anions  $\text{S}^{2-}$  react with cadmium

cations accumulated in the solution during the cathode polarization period and precipitate CdS by the reaction:



Simultaneously to anion reduction, the process reverse to the dissolution of cadmium electrodes takes place, namely the reduction of cadmium cations by reaction (3.12) resulting in the formation of the phase of metallic cadmium along with CdS:



The standard electrode potential of reaction (3.12) is  $E^\ominus = -0.4029 \text{ V}$  [15].

The diffraction patterns of nanocrystals produced with sodium sulfide solution as the electrolyte are shown in Fig. 4.

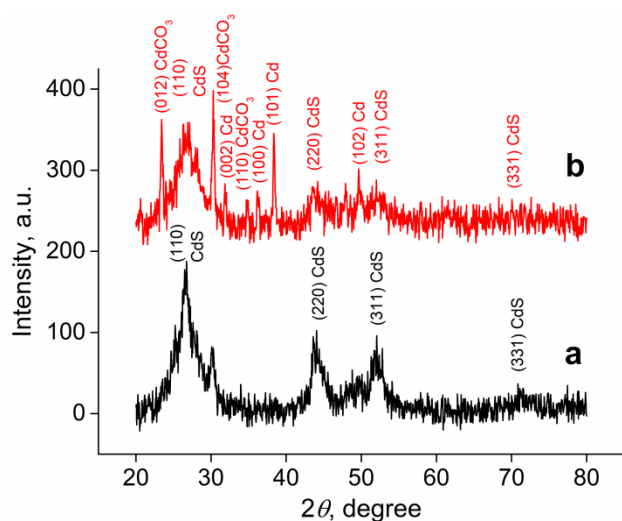


**Fig. 4** – Diffraction patterns of samples obtained by electrolytic method:  $t = 2 \text{ h}$ , electrolyte is  $\text{Na}_2\text{S}$  solution ( $c = 24.19 \text{ g/l}$ ) at  $T = 371 \text{ K}$  (a) and  $T = 292 \text{ K}$  (b)

Similarly to using sodium thiosulfate, the sample produced at  $T = 371 \text{ K}$  (Fig. 4a) is virtually pure CdS. The nanocrystal size estimated by Debye-Scherrer and Williamson-Hall methods was  $4.75 \text{ nm}$  and  $2.57 \text{ nm}$ , respectively, the value of the mechanical compression stress was  $\sigma = 6.87 \cdot 10^8 \text{ Pa}$ . A mixture of the nanocrystals of CdS, cadmium carbonate and metallic cadmium was obtained at  $T = 292 \text{ K}$  (Fig. 4b). The particle sizes calculated by Debye-Scherrer method are  $3.0 \text{ nm}$ ,  $35 \text{ nm}$ , and  $54 \text{ nm}$  for CdS,  $\text{CdSO}_3$ , and Cd, respectively. The Williamson-Hall calculations established the following parameters for CdS:  $D = 4.5 \text{ nm}$ ,  $\sigma = 6.8 \cdot 10^8 \text{ Pa}$ .

Raman spectra of CdS nanocrystals obtained from sodium thiosulfate solution are shown in Fig. 5. The spectra feature scattering bands with frequency positions of  $302 \text{ cm}^{-1}$ ,  $603 \text{ cm}^{-1}$ , and  $900 \text{ cm}^{-1}$ , with monotonously decreasing intensity. These bands are caused by scattering on the first-, second-, and third-order LO phonons, respectively, localized in nanocrystals.

Related Raman studies were performed in [16] where CdS nanoparticles were obtained by chemical reaction of the solutions of  $\text{Cd}(\text{NO}_3)_2$  and  $\text{Na}_2\text{S}$  in methanol. The samples were annealed at  $T = (473, 573, 673, 773) \text{ K}$ . It was determined that the intensity ratio

of the scattering bands  $I_{2LO}/I_{1LO}$  for the cubic modification varies within 0.2-0.5 as the particle size changes from  $5 \text{ nm}$  to  $10 \text{ nm}$ , and for the hexagonal CdS this ratio is  $> 1$ . In our case, the ratio of the noted integral intensities is  $\sim 0.3$  for both samples, thus confirming the conclusion about the formation of the cubic modification of CdS.

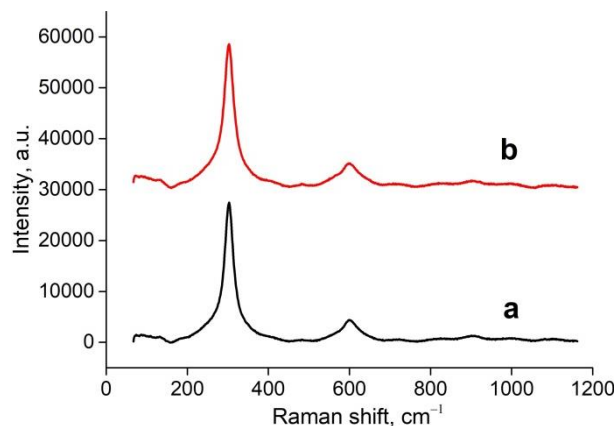


**Fig. 5** – Raman spectra ( $\lambda = 514.5 \text{ nm}$ ) of CdS nanocrystals obtained by electrolytic method:  $c = 12.5 \text{ g/l}$ ,  $j = 7.0 \cdot 10^{-3} \text{ A/cm}^2$ ,  $t = 3 \text{ h}$ , electrolyte is  $\text{Na}_2\text{S}_2\text{O}_3$  solution at  $T = 371 \text{ K}$  (a) and  $T = 292 \text{ K}$  (b)

The scattering bands of both samples at  $\nu = 302 \text{ cm}^{-1}$  have large FWHM, are asymmetrical with a clearly defined low-frequency shoulder. It was established that the peak width is  $36.3 \text{ cm}^{-1}$  and  $39.7 \text{ cm}^{-1}$  for samples produced at the electrolyte temperature of  $T = 371 \text{ K}$  and  $T = 292 \text{ K}$ , respectively. Such dependence may be caused by size effects, mechanical stress, or the presence of scattering bands due to surface optical and TO phonons. The size effect causes the shift of the scattering band to the low-frequency side and the increase of its width. Mechanical compression stress shifts the band to the high-frequency side, while the stretching stress shifts to the low-frequency side. The scattering band on the surface optical phonons lies between the TO and LO bands.

First-order Raman spectra of CdS nanocrystals in the region of LO phonons were analyzed in [17]. Multi-Lorentzian fitting used in the work took into account scattering by TO phonons, surface SO phonons, LO phonons, and high-frequency scattering (HFS) band that was likely caused by surface atoms of sulfur. Obtained results ( $\nu_{\text{TO}} = 255 \text{ cm}^{-1}$ ,  $\nu_{\text{SO}} = 284 \text{ cm}^{-1}$ ,  $\nu_{\text{LO}} = 302 \text{ cm}^{-1}$ ,  $\nu_{\text{HFS}} = 334 \text{ cm}^{-1}$ ) are similar to those obtained in this work using Gaussian fitting.

Quantum dots of cadmium sulfide and selenide deposited on silicon substrate were investigated in [18]. A low-frequency shift of the scattering bands on LO phonons was observed for both compounds. The authors performed theoretical frequency calculations depending on the quantum dot radius taking into account the presence of the surface phonon scattering band. It was determined that the decrease of the quantum dot radius from  $3 \text{ nm}$  to  $1.5 \text{ nm}$  should shift the scattering band frequency for CdS from  $302 \text{ cm}^{-1}$  to  $292 \text{ cm}^{-1}$ . For our samples, the frequency position does not change and equals  $302 \text{ cm}^{-1}$ .

CdS nanoparticles were produced in [19] by chemical precipitation of a cadmium salt and sodium sulfide. X-ray studies showed that obtained samples crystallize in the cubic structure with  $D \sim 3$  nm (by Debye-Scherrer formula). Williamson-Hall method showed that the nanoparticles are under compression stress (negative angular coefficient of the plot). Raman spectra were also investigated using excitation with  $\lambda = 514$  nm wavelength. The scattering band on LO phonons has frequency position  $\nu = 300$   $\text{cm}^{-1}$  and shows asymmetry in the low-frequency side. It was found that thermal annealing at  $T = 423$  K does not substantially affect Raman spectra.

Diffraction patterns of samples similar in composition to those shown in Fig. 1 and additionally annealed in a resistance electric furnace at  $T = 773$  K for 2 h are presented in Fig. 6. Material difference between the diffraction patterns is established. Specifically, the diffraction pattern in Fig. 6a contains many more and much narrower reflections than that of the unannealed sample in Fig. 1a. Comparing the diffraction pattern with the literature results [2, 20], we concluded that identified reflexes are typical of hexagonal CdS. Similar changes of the structure of nanocrystals upon annealing were described in [6].

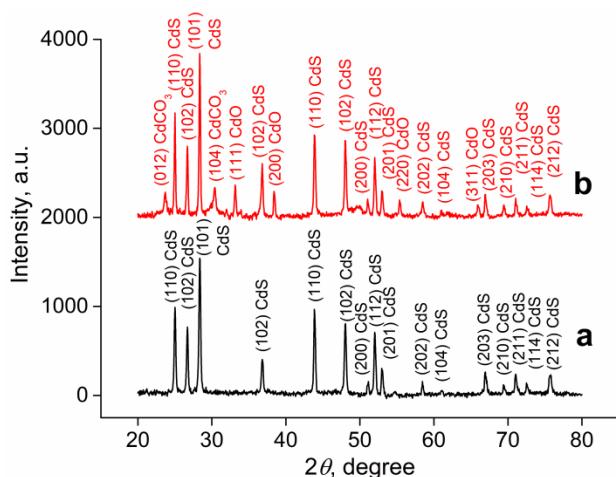
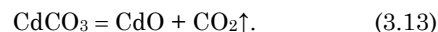


**Fig. 6** – Diffraction patterns of samples obtained by electrolytic method ( $t = 2$  h, electrolyte is  $\text{Na}_2\text{S}_2\text{O}_3$  solution ( $c = 12.5$  g/l) at  $T = 371$  K (a) and  $T = 292$  K (b) and annealed at  $T = 773$  K

Diffraction pattern of the sample obtained at  $T = 292$  K and annealed at  $T = 773$  K (Fig. 6b) contains reflections typical of the hexagonal CdS and low-intensity reflections belonging to cadmium carbonate ( $2\theta$  angles  $23^\circ$  and  $30^\circ$ ) and cadmium oxide (at  $33^\circ$ ,  $38^\circ$ ,  $55^\circ$ , and  $66^\circ$ ). The intensity of  $\text{CdCO}_3$  reflections is much lower

than the intensity of the same reflections in the original sample (Fig. 1b). This can be explained by the decomposition of cadmium carbonate during the annealing process:



Reaction (3.13) results in the reduction of calcium carbonate over time and the formation of cadmium oxide and carbon dioxide. Similar results were described in [10] upon the annealing of cadmium carbonate and electrolytic synthesis of cadmium compounds.

The dimension and mechanical stress of annealed nanocrystals were calculated by Debye-Scherrer and Williamson-Hall methods. For the CdS sample obtained at  $T = 292$  K and annealed at  $T = 773$  K these values are  $D = 45.9$  nm (Debye-Scherrer method);  $D = 65$  nm, tensile stress  $\sigma = 3.5 \cdot 10^7$  Pa (Williamson-Hall method). The nanocrystal sizes of the sample obtained at  $T = 292$  K and annealed at  $T = 773$  K are  $D = 76.5$  nm for CdS,  $D = 57.3$  nm for CdO,  $D = 26.2$  nm for  $\text{CdCO}_3$ .

#### 4. CONCLUSIONS

CdS nanocrystals of the cubic modification were obtained by the electrolytic method at various electrolyte temperatures. Solutions of sodium thiosulfate, sodium sulfite, and sodium sulfide in distilled water were used as electrolytes.

Using sodium thiosulfate solution, only CdS nanocrystals are produced at  $T = 371$  K, and the mixture of CdS and  $\text{CdCO}_3$  is obtained at  $T = 292$  K. The size of the synthesized CdS nanoparticles decreases from  $D \sim 3$  nm to  $D \sim 2$  nm as the temperature decreases from  $T = 371$  K to  $T = 292$  K. With sodium sulfite solution as the electrolyte, nanocrystals of CdS and Cd were obtained at either temperature. The use of sodium sulfide solution yields virtually pure CdS nanocrystals at  $T = 371$  K, and the mixture of CdS,  $\text{CdCO}_3$ , and Cd at  $T = 292$  K.

Annealing at  $T = 773$  K of CdS nanocrystals obtained from sodium thiosulfate solution causes the sphalerite-wurtzite phase transition.

The study of Raman spectra confirms the production of nanosized CdS crystals of the cubic modification.

#### ACKNOWLEDGEMENTS

Financial support was obtained within the frame of national projects of the Ministry of Education and Science of Ukraine. Project name: "Synthesis, physico-chemical and thermodynamic properties of nanosized and nanostructured materials for electrochemical systems", No. 0120U102184.

#### REFERENCES

1. A.A. Zarubanov, K.S. Zhuravlev, *Semiconductors* **49**, 380 (2015).
2. S. Khajuria, S. Sanotra, K. Heena, S. Anuraag, H.N. Sheikh, *Acta Chim. Slov.* **63**, 104 (2016).
3. J.M. Coronado, F. Fresno, M.D. Hernández-Alonso, R. Portela, *Design of Advanced Photocatalytic Materials for Energy and Environmental Applications* (London: Springer: 2013).
4. N. Memarian, *J. Nano-Electron. Phys.* **9** No 3, 03027 (2017).
5. Q. Zhang, Y. Zhang, S. Huang, X. Huang, Y. Luo, Q. Meng, D. Li, *Electrochem. Commun.* **12**, 327 (2010).
6. N.B. Danilevska, M.V. Moroz, A.V. Lysytsya, B.D. Nechyporuk, M.V. Prokhorenko, B.A. Tataryn, Fiseha Tesfaye, *J. Nano-Electron. Phys.* **11** No 1, 01015 (2019).
7. S.V. Volkov, E.P. Kovalchuk, V.M. Ogenko, O.V. Reshetnyak, *Nanochemistry. Nanosystems. Nanomaterials* (Kyiv: Naukova Dumka: 2008) [in Ukrainian].

8. L. Arunraja, P. Thirumorthy, A. Karthik, G. Sriram, V. Rajendran, L. Edwinpaul, *Synth. React. Inorg., Met.-Org., Nano-Met. Chem.* **46**, 1642 (2016).
9. N.S. Kozhevnikova, A.S. Vorokh, A.A. Uritskaya, *Russ. Chem. Rev.* **84**, 225 (2015).
10. N.B. Danilevska, M.V. Moroz, B.D. Nechyporuk, V.O. Yukhymchuk, N.E. Novoseletskiy, *J. Nano-Electron. Phys.* **8** No 2, 02041 (2016).
11. K. Ozga, J. Michel, B.D. Nechyporuk, J. Ebothé, I.V. Kityk, A.A. Albassam, A.M. El-Naggar, A.O. Fedorchuk, *Physica E* **81**, 281 (2016).
12. N.B. Danilevska, A.V. Lysytsya, M.V. Moroz, B.D. Nechyporuk, N.Yu. Novoseletskiy, B.P. Rudyk, *Tech. Phys.* **63**, 411 (2018).
13. V.D. Mote, Y. Purushotham, Bn. Dole, *J. Theor. Appl. Phys.* **6**, 6 (2012).
14. S. Adachi, *Handbook on Physical Properties of Semiconductors* (Springer Science & Business Media: 2004).
15. A.M. Sukhotin, *Reference Book on Electrochemistry* (Leningrad: Chemistry: 1981) [in Russian].
16. V. Sivasubramanian, A.K. Arora, M. Premila, C.S. Sundar, V.S. Sastry, *Physica E* **31**, 93 (2006).
17. V. Dzhagan, M. Valakh, N. Mel'nik, O. Rayevska, I. Lokteva, J. Kolny-Olesiak, D.R.T. Zahn, *Int. J. Spectrosc.* **2012**, 1 (2012).
18. W. Cheung, S. Montes, L. Zhang, I.O. Mondragon, A. Linares-Garsia, D. Bishel, *Proceedings of the International Scientific Conference: Quantum Dots and Nanostructures: Growth, Characterization, and Modeling XV* (San Francisco, USA) 10543 (2018).
19. R.R. Prabhu M. Abdul Khadar, *Bull. Mater. Sci.* **31**, 511 (2008).
20. C.F. Holder, R.E. Schaak, *ACS Nano* **13**, 7359 (2019).

### Вплив хімічного складу і температури електроліту на розмір та структуру нанокристалів сульфід кадмію, отриманих електролітичним методом

Н.Б. Данілевська<sup>1</sup>, М.В. Мороз<sup>2,3</sup>, Б.Д. Нечипорук<sup>1</sup>, С.Г. Гаєвська<sup>4</sup>, М.Ю. Новоселецький<sup>1</sup>, М.В. Прохоренко<sup>5</sup>, Н.П. Ярема<sup>5</sup>, В.О. Юхимчук<sup>6</sup>, Фісеха Тесфайе<sup>7</sup>, О.В. Решетняк<sup>3</sup>

<sup>1</sup> Рівненський державний гуманітарний університет, вул. Пластова, 31, 33000 Рівне, Україна

<sup>2</sup> Національний університет водного господарства і природокористування, вул. Соборна, 11, 33000 Рівне, Україна

<sup>3</sup> Львівський національний університет імені Івана Франка, вул. Кирила і Мефодія, 6, 79005 Львів, Україна

<sup>4</sup> Рівненський науково-дослідний експертно-криміналістичний центр, вул. Гагаріна, 31, 33003 Рівне, Україна

<sup>5</sup> Національний університет "Львівська політехніка", вул. Степана Бандери, 12, 79013 Львів, Україна

<sup>6</sup> Інститут фізики напівпровідників імені В.С. Лашкарьова НАН України, пр. Науки, 41, 03028 Київ, Україна

<sup>7</sup> Університет Академія Або, вул. Пііспанкату, 8, 20500 Турку, Фінляндія

Нанокристали сульфід кадмію (CdS) отримано електролітичним методом в скляному електролізері з кадмієвими електродами. В якості електроліту використано розчини  $\text{Na}_2\text{S}_2\text{O}_3$ ,  $\text{Na}_2\text{SO}_3$  та  $\text{Na}_2\text{S}$  в дистильованій воді. При електролізі температура електроліту становила  $T = 292$  К або  $371$  К, час синтезу  $t = 2$ - $3$  год, напруга між електродами  $U \sim 10$  В, а густина струму  $j = 7.0 \cdot 10^{-3}$  А/см<sup>2</sup>. Встановлено, що хімічний склад отриманих фаз залежить від електроліту та температури синтезу. Сульфід кадмію, як однофазний продукт реакції, отримано з розчинів  $\text{Na}_2\text{S}_2\text{O}_3$  та  $\text{Na}_2\text{S}$  при  $T = 371$  К. При використанні інших електролітів та температур окрім сульфід кадмію отримано додаткові фази  $\text{CdCO}_3$  та  $\text{Cd}$ . Розмір синтезованих наночастинок, їхню кристалічну структуру визначено за даними рентгенівського дифракційного аналізу з використанням формул Дебая-Шеррера і Вільямсона-Холла. При пониженні температури розчину  $\text{Na}_2\text{S}_2\text{O}_3$  від  $T = 371$  К до  $T = 292$  К розміри синтезованих наночастинок CdS зменшуються. Для кубічної та гексагональної модифікацій нанокристалів CdS розраховано значення механічних напружень. Досліджено спектри комбінаційного розсіювання світла нанокристалів сульфід кадмію, отриманих з розчину  $\text{Na}_2\text{S}_2\text{O}_3$ . Встановлено наявність смуг розсіювання з частотним положенням  $\nu = 302$  см<sup>-1</sup>,  $603$  см<sup>-1</sup> та  $900$  см<sup>-1</sup>, інтенсивність котрих монотонно зменшується. Детально проаналізовано отримані експериментальні результати та опубліковані літературні дані. Встановлено, що фазовий перехід сфалерит-вурцит відбувається при відпалі нанокристалів CdS при  $T = 773$  К. Результатом фазового переходу є збільшення розмірів та зменшення механічних напружень нанокристалів сульфід кадмію.

**Ключові слова:** Сульфід кадмію, Рентгеноструктурні дослідження, Розміри наночастинок, Комбінаційне розсіювання світла.